Heliyon 10 (2024) e40319

Contents lists available at ScienceDirect

Heliyon

journal homepage: www.cell.com/heliyon

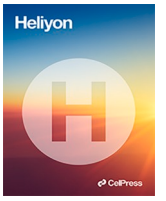

Research article

Efficient adsorptive removal of levofloxacin using sulfonated graphene oxide: Adsorption behavior, kinetics, and thermodynamics

Chironjit Kumar Shaha [a,b], Subarna Karmaker [a], Tapan Kumar Saha [a,*,1]

[a] Department of Chemistry, Jahangirnagar University, Savar, Dhaka, 1342, Bangladesh
[b] Veterinary Drug Residue Analysis Division, Institute of Food and Radiation Biology, Atomic Energy Research Establishment (AERE), Gonokbari, Savar, Dhaka, 1349, Bangladesh

ARTICLE INFO

Keywords:
Sulfonated graphene oxide
Levofloxacin
Adsorption
Kinetics
Isotherm

ABSTRACT

Water pollution by antibiotic residues poses a potential threat to environmental and human health. Graphene-based materials are highly stable, recyclable and effective adsorbents for efficiently removing antibiotics from polluted water. In this study, the adsorption behavior of levofloxacin onto sulfonated graphene oxide (SGO) was investigated by varying the contact period, solution pH, adsorbent quantity, levofloxacin concentration, inorganic ions, and solution temperature. Spectroscopic and microscopic techniques were employed to confirm the adsorptive interaction between levofloxacin and SGO. The adsorption process was most accurately characterized by the pseudo-second-order kinetic model and the Langmuir isotherm model, as indicated by their high correlation coefficients (R^2) and low root-mean-square error (RMSE) values. The maximal quantity of levofloxacin that can be adsorbed onto SGO was determined to be 1250 μmol/g at pH 4 and 25 °C using the Langmuir model. Thermodynamic studies reveal that the process of levofloxacin adsorption onto SGO is endothermic and spontaneous in nature. Taking into consideration the results of adsorption, desorption and regeneration studies, it is proposed that SGO can be applied as an economic viable agent for the adsorptive removal of levofloxacin from the aqueous environment.

1. Introduction

Contamination of water sources with antibiotics is one of the top environmental concerns around the world. Various classes of antibiotics have been found in water bodies, with concentrations ranging from less than 1 ng/L to 100 μg/L [1]. The entry pathways of antibiotics to the water bodies are excretions from humans [2–4], poor disposal of unused antibiotics [5], hospital effluents [6], animal farming [7,8], plant production [9], aquaculture [10], and pharmaceutical effluents [11–13]. Antibiotic contaminated water resources are considered as potential reservoirs of antibiotic resistant bacteria [14,15]. Therefore, it is essential to develop a simple and cost-effective method for removing antibiotic residues from the aquatic environment.

Levofloxacin (Fig. 1), a third generation antibiotic of fluoroquinolone group, is consumed by both humans [16] and farm animals

* Corresponding author.
E-mail addresses: chironjit39@gmail.com (C.K. Shaha), ksubarna_ju@yahoo.com (S. Karmaker), tksaha_ju@yahoo.com (T.K. Saha).
[1] https://juniv.edu/teachers/tksaha_ju.

https://doi.org/10.1016/j.heliyon.2024.e40319
Received 3 June 2024; Received in revised form 3 July 2024; Accepted 8 November 2024
Available online 10 November 2024

[17] for the treatment of bacterial infectious diseases. A pharmacokinetic study revealed that about 80 % of the ingested levofloxacin is excreted as parent molecule in the urine [18]. Levofloxacin residues were detected at concentrations ranging from 123 to 209 ng/L in drinking water treatment plants in Baghdad city [19], from 3600 to 6800 ng/L in influents at a sewage treatment plant in Kyoto, Japan [20], and from 34 to 438 ng/L in wastewater effluents from a wastewater treatment plant in Portugal [21]. It has been reported that levofloxacin at a concentration of 5 μg/L significantly altered the structure of the prokaryotic microbial community [22]. This is due to the fact that its residue can contribute to bacterial resistance and negatively impact aquatic ecosystems [23]. For example, levofloxacin can be fatal to fish embryos within 24 h of exposure. Furthermore, it can be biomagnified and bioaccumulated when exposed aquatic species enter the food chain, and it also inhibits algal growth in aquatic environments [24]. Orzoł and Piotrowicz-Cieślak [25] studied the effects of levofloxacin toxicity on yellow lupin plants. Lupin is a commonly used fodder crop, and biochemical contaminants that accumulate in it can enter food chains involving farm animals. The findings revealed that levofloxacin's toxicity was primarily evident through alterations in the protein profile. Morphologically, levofloxacin soil contamination could lead to over a 50 % reduction in lupin root and shoot growth and a comparable decrease in seedling fresh mass.

Several methods have been employed to remove levofloxacin from aqueous solutions, including nano-filtration [21], photocatalytic degradation [26,27], sonocatalytic degradation [28], advanced oxidation processes [29,30], electrochemical treatment [31], coagulation–flocculation [32], and adsorption [24,33]. Among these, adsorption is considered a very simple and cost-effective technique for treating aqueous solutions contaminated with various organic pollutants, including levofloxacin [24,33–35]. Various carbon-based adsorbents have been used for this purpose, such as graphene oxide [36], FXM hydrogel (Fe(III)-tartaric acid/xanthan gum/graphene oxide/polyacrylamide) [37], granular activated carbon [38], cellulose nanocrystals/graphene oxide [39], graphene nanoplatelets [40], rice husk biochar [41], and multi-walled carbon nanotubes [42].

Over the years, carbon-based materials have been widely used to effectively remove hazardous substances from wastewater, demonstrating their permanent importance in environmental remediation efforts. Recently, graphene oxide (GO) has attracted significant scientific attention in adsorption technology due to its modifiable surface functionalities and high specific surface area [43–50]. GO contains hydroxyl, epoxy, carbonyl, and carboxyl groups attached to its edges and surface [51]. It consists of both sp^2 and sp^3 hybridized domains. GO demonstrates excellent adsorption capacity for various water pollutants, mainly due to electrostatic and π-π stacking interactions [52,53]. It is highly stable and can be recycled with minimal loss in adsorption capacity [54]. Recent studies indicate that incorporating sulfonate groups into graphene oxide substantially improves its ability to adsorb antibiotics [55].

These findings led us to investigate the ability of sulfonated graphene oxide (SGO) to remove levofloxacin from aquatic environments. The study investigated the adsorption of levofloxacin onto SGO, focusing on the effects of contact time, solution pH, adsorbent dosage, levofloxacin concentration, inorganic ions, and solution temperature. The adsorptive interaction between levofloxacin and SGO was confirmed using Fourier transform infrared (FTIR) analysis, scanning electron microscope (SEM) imaging, and energy dispersive X-ray spectroscopy (EDX) evaluation. The adsorption kinetics were examined using several models, including pseudo-first-order, pseudo-second-order, Elovich, film diffusion, and intraparticle diffusion models. To evaluate the adsorption equilibrium data, various isotherm models such as Freundlich, Temkin, Dubinin-Radushkevich, and Langmuir were utilized. Additionally, thermodynamic and activation parameters were assessed. The study also investigated desorption of levofloxacin from antibiotic-loaded SGO and evaluated the recyclability of SGO as an adsorbent material to assess its economic feasibility for wastewater treatment applications.

2. Experimental

2.1. Chemicals

Graphite and levofloxacin were acquired from Sigma-Aldrich and used as received. Levofloxacin was dissolved in water to prepare a stock solution of 5 mmol/L. The entire investigation was conducted using deionized water. All other chemicals used in this study were analytical grade.

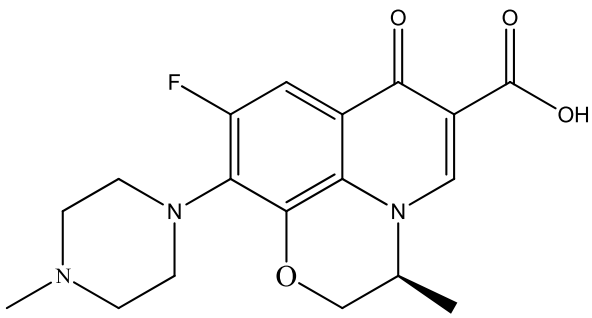

Fig. 1. Chemical structure of levofloxacin.

2.2. Synthesis and characterization of sulfonated graphene oxide (SGO)

SGO was synthesized from graphite flakes using the Improved Hummers' method with a slight modification [56]. In summary, graphite flake (3.0 g) was slowly combined with a mixture of sulfuric acid (18.4 mol/L, 360 mL) and phosphoric acid (14.6 mol/L, 40 mL) after stirring for 30 min. Under continuous magnetic stirring at 30 °C, 18.0 g of solid $KMnO_4$ was steadily introduced into the mixture. Ice water (400 mL) was introduced to the mixture after stirring for 24 h. Hydrogen peroxide (9.8 mol/L, 3 mL) were added to the mixture. A spontaneous sedimentation process was employed to separate the product from the mixture. The solid product underwent sequential washing with HCl (7.7 mol/L), water, ethanol, and ether. The obtained material was dried in an oven at 60 °C.

The FTIR spectrum of SGO and levofloxacin-loaded SGO was measured in KBr at wavenumbers between 400 and 4000 cm^{-1} using a Shimadzu IRPrestige-21 FTIR Spectrophotometer. SEM imaging and EDX analysis of SGO before and after levofloxacin adsorption were conducted with an Oxford EDS/EBSD system integrated with a Thermo Fisher Helio G4 Xe plasma FIB/SEM system. The accelerating voltage used for acquiring SEM images and EDX data was 20 kV.

2.3. Adsorption and desorption experiments

Adsorption experiment was conducted in batch mood in a 125 mL stoppered bottle containing 10 mg of SGO in 50 mL of aqueous levofloxacin solution (50 μmol/L) [57]. The pH of the levofloxacin solution was adjusted to 4.0 using either 0.1 mol/L HCl or NaOH solution, with the assistance of a digital pH meter (HACH, HQ11D). A temperature-controlled mechanical shaker was used to agitate the mixtures at 150 rpm for 240 min at room temperature (25 °C) in order to achieve equilibrium. Each sample container was tightly sealed to prevent water evaporation at elevated temperatures. In order to separate the adsorbent material from the mixtures after a predetermined period, the samples were centrifuged at 9000 rpm for 1 min using a Flexpin Benchtop Centrifuge, LC 200, Japan. Levofloxacin concentration in the upper portion of the solution was determined utilizing a spectrophotometer (Shimadzu UV-1900i, Shimadzu, Japan) at λ_{max}: 292 nm (pH 2–6) and 289 nm (pH 7–11). The levofloxacin exhibited an estimated molar absorptivity of 26.0 $\times 10^3$ L/mol.cm at 292 nm and 25.0 $\times 10^3$ L/mol.cm at 289 nm in aqueous medium. The adsorption capacity of levofloxacin onto SGO at time t, q_t (μmol/g) was estimated utilizing the following formula [57]:

$$q_t = \frac{(C_0 - C_t)}{m} \times V \tag{1}$$

where, C_0 (μmol/L) denotes the initial concentration of levofloxacin at zero time and C_t (μmol/L) denotes the concentration of levofloxacin at time *t*; *V* (L) represents the solution volume and *m* (g) represents the mass of SGO. The adsorption kinetics of levofloxacin onto SGO were also investigated varying solution pHs (2–11), dosages of SGO (0.003–0.02 g), levofloxacin concentrations (10–100 μmol/L), cations (Na^+, K^+, Mg^{2+}, and Ca^{2+}), and temperatures (25, 30, 35, and 40 °C), respectively.

The equilibrium adsorption of levofloxacin onto SGO was performed in an aqueous solution with a pH of 4 at different temperatures (25, 30, 35, and 40 °C). The adsorption capacity of SGO, q_e (μmol/g), and the percentage of antibiotic removal at equilibrium were determined using the following equations [57]:

$$q_e = \frac{(C_0 - C_e)}{m} \times V \tag{2}$$

$$\text{Levofloxacin removal } (\%) = \frac{(C_0 - C_e)}{C_0} \times 100 \tag{3}$$

where the variable *Ce* (μmol/L) represents the equilibrium concentration of levofloxacin; C_0, *V*, and *m* have the identical significance as previously stated.

The desorption kinetics of levofloxacin from levofloxacin-loaded SGO were investigated in a solution containing 1 mol/L HCl in dimethylformamide (DMF). Initially, levofloxacin was loaded onto SGO under optimal adsorption conditions. The SGO loaded with levofloxacin was isolated from the adsorption medium by centrifugation at 9000 rpm and cleaned with water. After being thoroughly dried at 60 °C in an oven, the levofloxacin-loaded SGO was used for a desorption experiment. For the desorption study, 10 mg of levofloxacin-loaded SGO was dispersed in a 50 mL solution of acidic DMF, and the mixture was agitated on a mechanical shaker until equilibrium desorption was achieved. The quantity of desorbed levofloxacin in the acidic DMF solution was measured using a UV–Vis spectrophotometer. The regenerated SGO was carefully purified with deionized water until it reached a neutral pH. It was then dried at 100 °C, weighed, and reused in subsequent adsorption experiments. This regeneration and reuse process was repeated up to five cycles. In this study, all experimental data are presented as the average of two measurements.

2.4. Error analysis

Root-mean-square error (RMSE) is a commonly used statistical technique for evaluating the disparity between the predicted values of experimental and model (kinetic and isotherm) data [58]. In the present investigation, the suitability of the implemented theoretical models was assessed utilizing the following formula,

$$\mathrm{RMSE} = \sqrt{\frac{1}{N-p}\sum_{i=1}^{N}\left(q_{exp}-q_{cal}\right)^2} \quad (4)$$

The variable q_{exp} represents the experimental response value, while q_{cal} represents the model predicted response value. The parameter of kinetic or isotherm models is denoted by p, while N represents the number of experimental trials.

3. Results and discussion

3.1. Implications of contact time

The effect of contact time on the adsorption kinetics of levofloxacin (50 μmol/L) onto SGO was examined in an aqueous environment at pH 4.0 and 25 °C. The results of varying contact time are shown in Fig. 2. Fig. 2a displays the typical UV–visible absorption spectra of levofloxacin during its adsorption onto SGO in an aqueous medium. As contact time increased, the absorbance value of levofloxacin at 292 nm steadily decreased. The adsorption process was rapid during the first 30 min (Fig. 2b) and then slowed down, eventually reaching equilibrium at 60 min. The initial rapid adsorption of levofloxacin onto SGO is presumably the result of electrostatic interactions between the two [55,59]. Once the surface of SGO became saturated with the antibiotic, levofloxacin molecules began to diffuse into the pores of SGO, causing the adsorption rate to gradually decrease. Similar observations were noted for the adsorption of sparfloxacin onto SGO [55] and cefixime onto chitosan [57] in aqueous solutions. For further studies, a contact period of 240 min was chosen to ensure complete adsorption equilibrium.

3.2. Implications of solution pH

The uptake of levofloxacin by SGO is significantly influenced by the solution pH, as it governs both the surface charge of SGO and the ionization states of levofloxacin molecules in the aqueous solution. SGO exhibits a negative surface charge in aqueous solution when the pH exceeds its pH_{PZC} value of 2.5 [55]. Levofloxacin possesses two distinct acid dissociation constants ($pKa_1 = 5.59$ and $pKa_2 = 7.94$), allowing it to adopt various configurations—cationic ($pH < pKa_1$), anionic ($pH > pKa_2$), or neutral ($pKa_1 < pH < pKa_2$)—depending on the solution pH [60]. Thus, the ionization states of levofloxacin and SGO in an aqueous solution are markedly influenced by pH. Fig. 3 depicts the influence of solution pH, ranging from 2 to 11, on the adsorption of levofloxacin with SGO. The pH investigation revealed that the q_e value increased as the solution's pH increased from 2 to 3, remained constant until reaching pH 6, and thereafter decreased significantly for pH values exceeding 6. The highest quantity of levofloxacin adsorbed onto SGO was measured to be 232.5 μmol/g at a solution pH of 4.0. The low adsorption capacity at pH 2 may be ascribed to an electrostatic repulsion between the positively charged SGO surface ($pH < pH_{PZC}$) and the protonated levofloxacin molecules ($pH < pK_{a1}$). In a strongly acidic adsorption medium, the competition between H^+ ions and levofloxacin molecules for binding sites on the SGO surface may restrict the q_e value of SGO [61]. The decrease in q_e value at higher pH levels can be attributed to two main factors: firstly, the repulsion between deprotonated levofloxacin molecules ($pH > pKa_2$) and the negatively charged SGO surface ($pH > pH_{PZC}$), and secondly, the competition between OH^- ions and deprotonated levofloxacin molecules for surface binding sites on the SGO [55]. Similar results were noted when sparfloxacin was adsorbed onto SGO [55] and mGOCP [61], and when cefixime was adsorbed onto chitosan [57] in aqueous solutions. Consequently, the subsequent experiments were carried out in aqueous solution with a pH of 4.0.

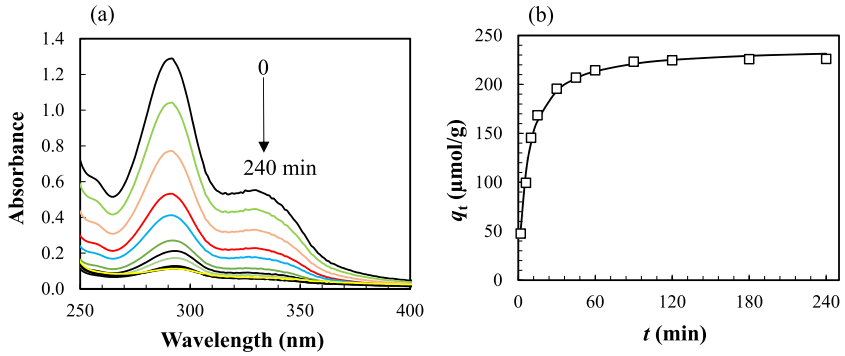

Fig. 2. (a) Typical changes in UV–visible absorption spectra of levofloxacin at various time intervals during adsorption onto SGO in aqueous solution at 25 °C. The spectra were taken at 0, 2, 6, 10, 15, 30, 45, 60, 90, 120, 180, and 240 min, respectively ($[Levofloxacin]_0$: 50 μmol/L; solution volume: 0.05 L; pH 4.0; SGO: 0.01 g). (b) The variations in the adsorption capacity (q_t) of levofloxacin onto SGO as a function of contact time, t, in aqueous solution at 25 °C. The solid line represents the adsorption kinetic traces modeled using the pseudo-second-order equation (Eq. 7) and the corresponding $q_{e(cal)}$ and k_2 values found in Table 1.

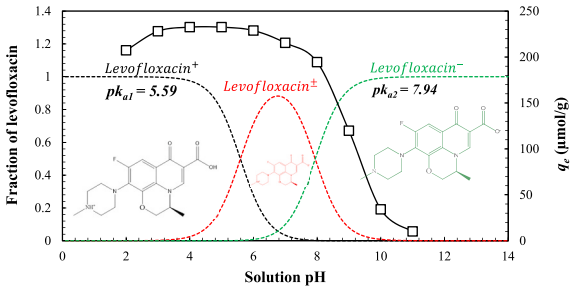

Fig. 3. The impact of solution pH on levofloxacin uptake onto SGO ([Levofloxacin]$_0$: 50 μmol/L; solution volume: 0.05 L; SGO: 0.010 g; pH: 2–11; temperature: 25 °C).

3.3. The impact of dosage

To examine the impact of adsorbent dosage, the extent of levofloxacin adsorption was evaluated by varying the amount of SGO from 3 to 20 mg in an aqueous solution at pH 4.0. Fig. 4 shows that the proportion of levofloxacin removal increased from 69.88 % to 93.23 % as the adsorbent dosage was increased from 3 to 20 mg, while keeping other adsorption parameters constant. This can be attributed to the increase in available adsorption sites and the subsequent expansion of the surface area of SGO. Conversely, there was a significant decrease in the adsorption capacity (q_e) from 575.64 to 115.19 μmol/g as the amount of SGO increased (Fig. 4). As the adsorption capacity (q_e) is inversely proportional to adsorbent mass (m), an increase in adsorbent mass leads to a decrease in q_e values. Similar results were observed in comparable experiments where sparfloxacin was adsorbed onto SGO [55], and sawdust treated with hexadecylpyridinium bromide and the marine alga *Porphyra yezoensis* Ueda were used to extract the dyes allura red AC [62] and Congo red [63] from aqueous solutions, respectively.

3.4. Effects of concentration of levofloxacin

To explore the kinetics of adsorption, the adsorption capacity was evaluated by altering the antibiotic concentration in the solution, ranging from 10 to 100 μmol/L. Fig. 5 illustrates the relationship between the adsorption of levofloxacin onto SGO (q_t, μmol/g) and the interaction time (t, min) at various concentrations of levofloxacin. With an increase in the concentration of levofloxacin, both the initial adsorption rate (h, μmol/g min) and the quantity of antibiotic adsorption onto SGO (q_e, μmol/g) were increased. As depicted in Fig. 5, the q_e value increased from 39.42 to 388.27 μmol/g when the concentration of levofloxacin increased from 10 to 100 μmol/L. The findings indicate that the antibiotic concentration in the adsorption medium serves as a critical driving force, overcoming any resistance to mass transfer between the adsorbate and the adsorbent, thus facilitating the adsorption process [64]. Similar results were also observed when sparfloxacin was adsorbed onto SGO [55], and when cefixime [57], remazol brilliant violet (RBV) [65], and reactive black 5 (RB5) [66] were removed from aqueous solutions using chitosan.

3.5. The impact of salts

The impact of inorganic salts on the adsorptive removal of levofloxacin was investigated by the addition of 0.1 mol/L of Na_2SO_4, K_2SO_4, $CaSO_4$, and $MgSO_4$ salts successively in adsorption medium. As illustrated in Fig. 6, the presence of inorganic ions in the

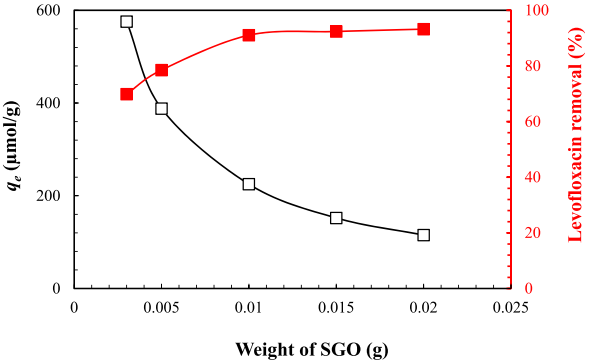

Fig. 4. The changes in the equilibrium adsorption capacity (q_e: □) and the removal percentage (%: ■) of levofloxacin onto SGO were investigated using different amounts of SGO in an aqueous medium ([Levofloxacin]$_0$: 50 μmol/L; solution volume: 0.05 L; SGO: 0.003–0.020 g, pH: 4.0, temperature: 25 °C).

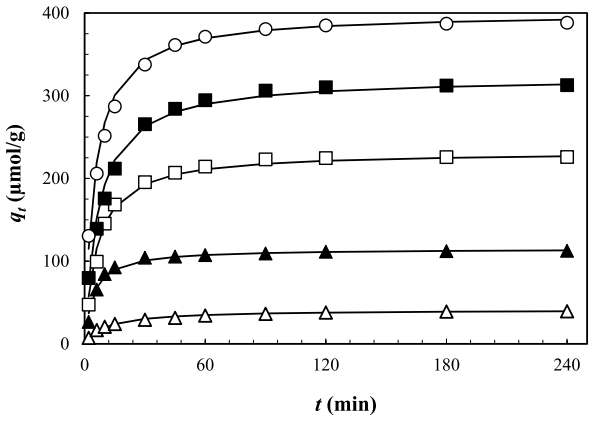

Fig. 5. The relationship between adsorption capacity (q_t) of levofloxacin onto SGO and contact time (t) at various concentrations of levofloxacin in aqueous solution. (Solution volume: 0.05 L; SGO: 0.010 g; temperature: 25 °C; pH: 4.0; $[Levofloxacin]_0$: Δ: 10 μmol/L; ▲: 25 μmol/L; □: 50 μmol/L; ■: 75 μmol/L; ○: 100 μmol/L). Equation (7) was utilized to numerically simulate each line, with the values of $q_{e(cal)}$ and k_2 being provided in Table 1.

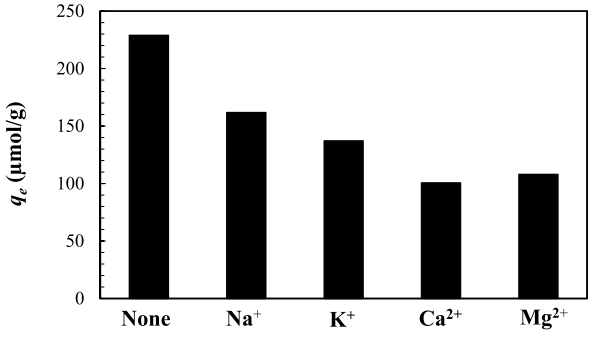

Fig. 6. Variations in the equilibrium adsorption capacity (q_e) of levofloxacin onto SGO in an aqueous solution containing different inorganic ions. ($[Levofloxacin]_0$: 50 μmol/L, solution volume: 0.05 L, SGO: 0.010 g, pH: 4.0, temperature: 25 °C).

levofloxacin solution (pH 4.0) hinders the absorption capacity of SGO [67]. The inhibition of levofloxacin adsorption onto SGO in aqueous solution by metal ions follows the order: $Ca^{2+} > Mg^{2+} > K^+ > Na^+$. This may be due to the aggregation of SGO in solution induced by the presence of inorganic ions in the solution. The metal ions induce the aggregation of GO in aqueous solution in the following order: $Ca^{2+} > Mg^{2+} > K^+ > Na^+$ [68]. Given the significant impact of metal ions on the adsorption process, it is plausible that levofloxacin is adsorbed onto SGO through a mechanism involving electrostatic outer sphere adsorption. Similar results were observed with the adsorption of sparfloxacin onto SGO in an aqueous solution [55].

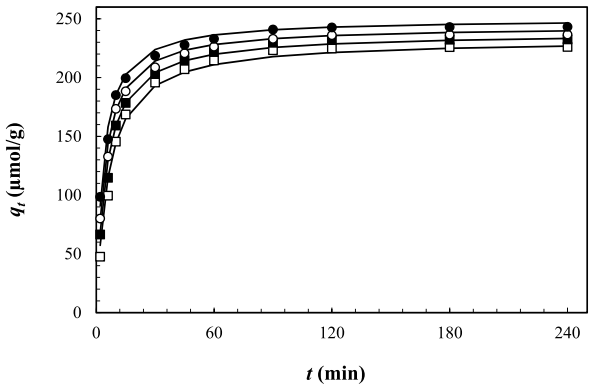

Fig. 7. The variation in the adsorption capacity of levofloxacin (q_t) onto SGO with contact time (t) in aqueous solution (pH 4.0) at distinct temperature conditions ($[Levofloxacin]_0$: 50 μmol/L; solution volume: 0.05 L; SGO: 0.010 g; Temperature: □: 25 °C; ■: 30 °C; ○: 35 °C; ●: 40 °C, respectively). Equation (7) was employed to simulate each line, with the $q_{e(cal)}$ and k_2 values listed in Table 1.

3.6. The implications of temperature

Study of the temperature effect is essential for the design of all bulk experiments. Adsorption of levofloxacin onto SGO was conducted at varying temperatures. The effects of temperature are illustrated in Fig. 7. The initial adsorption rate of levofloxacin, h (μmol/g min), increased from 38.02 μmol/g min to 71.43 μmol/g min with rising solution temperature from 25 °C to 40 °C (Table 1). This phenomenon may be attributed to the high dispersion of SGO in aqueous solutions at elevated temperatures. The equilibrium uptake capacity, q_e (μmol/g), of levofloxacin increased from 225.96 to 243.08 μmol/g with rising temperature from 25 °C to 40 °C. This occurrence might be ascribed to either an increase in the number of active binding sites accessible on the SGO surface or an enhancement in the diffusion rate of levofloxacin [67]. It is well known that the diffusion rate of adsorbate molecules across the surface layer and into the inner cavities of the adsorbent accelerates with increasing solution temperature. Similar observations were previously reported for the adsorption of sparfloxacin onto SGO [55], as well as for the adsorption of RB5 [66], VO(tpps) [69], and Zn (tpps) [70] molecules onto chitosan in aqueous solutions.

3.7. Kinetic simulation

The adsorption kinetics and mechanism of levofloxacin onto SGO were assessed employing the pseudo-first-order [71], pseudo-second-order [72], Elovich [73], film diffusion [74] and intraparticle diffusion [75] models, respectively. The linear equation representing the pseudo-first-order kinetic model can be expressed as follows:

$$\log (q_e - q_t) = \log q_e - \frac{k_1}{2.0303} t \tag{5}$$

In this context, k_1 (1/min) denotes the rate constant for the pseudo-first-order kinetic model, which can be determined by utilizing the slope of a linear plot of $\log(q_e - q_t)$ versus t.

The linear and nonlinear forms of pseudo-second-order kinetic model are represented by the subsequent formulas:

$$\frac{t}{q_t} = \frac{1}{k_2 q_e^2} + \frac{1}{q_e} t \tag{6}$$

$$q_t = \frac{k_2 q_e^2 t}{(1 + k_2 q_e t)} \tag{7}$$

In this context, k_2 (g/μmol min) represents the adsorption rate constant for the pseudo-second-order kinetic model. Using the intercept and slope of a plot $\frac{t}{q_t}$ versus t, the values of k_2 and q_e were computed. The initial uptake rate, h (μmol/g min), was estimated by the following equation:

Table 1
Summary of kinetic parameters of adsorption process at various levofloxacin concentrations and solution temperatures.

Parameters		[Levofloxacin]$_0$ (μmol/L)					Temperature (°C)			
		10	25	50	75	100	25	30	35	40
$q_{e(exp)}$	(μmol/g)	39.42	112.50	225.96	312.89	388.27	225.96	232.31	236.54	243.08
Pseudo-First-Order Kinetic Model										
$k_1 \times 10^{-3}$	(1/min)	23.30	27.50	37.40	33.50	30.40	37.40	38.60	37.60	37.50
$q_{e(cal)}$	(μmol/g)	24.31	36.78	119.46	169.03	158.95	119.46	111.94	101.93	91.63
R^2		0.9891	0.9233	0.9851	0.9832	0.9577	0.9851	0.9755	0.9753	0.9729
RMSE		16.52	80.69	113.08	151.84	242.58	113.08	127.93	144.45	162.60
Pseudo-Second-Order Kinetic Model										
$k_2 \times 10^{-3}$	(g/μmol min)	2.24	2.06	0.70	0.46	0.50	0.70	0.84	0.98	1.14
h	(μmol/g min)	3.80	27.25	38.02	47.62	80.65	38.02	47.85	58.48	71.43
$q_{e(cal)}$	(μmol/g)	41.15	114.94	232.56	322.58	400.00	232.56	238.10	243.90	250.00
R^2		0.9996	0.9999	0.9997	0.9998	0.9999	0.9997	0.9999	0.9999	0.9999
RMSE		1.07	4.02	6.82	8.66	10.02	6.82	5.54	4.58	5.28
Elovich Kinetic Model										
$\alpha \times 10^3$	(μmol/g min)	0.013	0.162	0.132	0.168	0.482	0.13	0.23	0.45	0.98
$\beta \times 10^{-3}$	(g/μmol)	145.89	62.24	26.57	19.17	17.92	26.57	28.59	31.26	33.92
R^2		0.9817	0.8320	0.9058	0.9385	0.9291	0.9058	0.9062	0.8982	0.8957
RMSE		1.49	11.48	19.30	21.23	24.51	19.30	17.89	17.12	15.99
Activation Parameters										
E_a	(kJ/mol)						24.98			
R^2							0.9988			
$\Delta G^{\ddagger}$	(kJ/mol)						56.72	57.30	57.87	58.45
$\Delta H^{\ddagger}$	(kJ/mol)						22.45			
$\Delta S^{\ddagger}$	(J/mol K)					−115.03				
R^2							0.9985			

$$h = k_2 q_e^2 \tag{8}$$

The equation of Elovich kinetic model is represented as follows:

$$q_t = \frac{1}{\beta}\ln(\alpha\beta) + \frac{1}{\beta}\ln t \tag{9}$$

The variables α (mol/g min) and β (g/μmol) represent the initial rate of levofloxacin adsorption and the extent of surface coverage along with activation energy, respectively. The values of α and β were estimated using the plot of q_t versus ln*t*.

Table 1 displays the adsorption parameter values obtained from the fitted kinetic models. The R^2 values obtained from the pseudo-second-order kinetic model (≥0.9996) were markedly higher compared to those of the pseudo-first-order (≤0.9891) and Elovich (≤0.9817) kinetic models. The experimental $q_{e(exp)}$ values showed a high degree of agreement with the calculated $q_{e(cal)}$ values obtained from the pseudo-second-order kinetic model (Table 1). Furthermore, the RMSE values for the pseudo-second-order kinetic model (1.07–10.02) were significantly lower compared to those of the pseudo-first-order model (16.52–242.58) and the Elovich model (1.49–24.51). These results indicate that the kinetic data of levofloxacin adsorption onto SGO were accurately described by the pseudo-second-order kinetic model. Similar phenomena were observed in the adsorption of sparfloxacin onto SGO [55] and cefixime onto chitosan [57] in aqueous solutions.

The mathematical representation of the film diffusion model can be expressed by the following formula:

$$\ln(1 - F) = -k_{fd}t \tag{10}$$

$$F = \frac{q_t}{q_\infty} \tag{11}$$

where k_{fd} (1/min) denotes the rate constant of the film diffusion model, *F* represents the degree of attainment towards equilibrium, and q_∞ (μmol/g) represents the amount of levofloxacin adsorbed after infinite time. The value of k_{fd} was determined from the ln(1-*F*) *vs*. *t* plot. Detailed results are provided in Table 2.

The intraparticle diffusion model is often utilized to describe the process of solute transport within porous materials. The equation representing this model is typically expressed as:

$$q_t = k_{id}t^{0.5} + I \tag{12}$$

where, k_{id} (μmol/g $min^{0.5}$) represents the rate at which solute molecules diffuse into the interior of the adsorbent particles and *I* (μmol/g) is associated to the thickness of boundary layer. As depicted by the multilinearity observed in the q_t versus $t^{0.5}$ plots in Fig. 8, the adsorption of levofloxacin proceeds through three distinct phases. Initially, levofloxacin molecules are transported from the liquid phase to the surface of SGO via diffusion across a boundary layer. Subsequently, internal diffusion takes place in the second and third phases, where levofloxacin molecules penetrate into the capillaries of SGO from its external surface [76]. The diffusion rates (k_{id1}, k_{id2}, and k_{id3}) were calculated based on the slopes of the respective lines in Fig. 8. The values for k_{id1} are higher than those for k_{id2} and k_{id3} (Table 2), indicating that levofloxacin was rapidly adsorbed onto the external surface of SGO. These three linear segments collectively indicate that the sorption of levofloxacin onto SGO involves both surface sorption and intraparticle diffusion mechanisms. Additionally, since the values of *I* are non-zero (Table 2), it can be assumed that intraparticle diffusion is not the sole rate-controlling step. Previously, it was noted that the adsorption of levofloxacin onto FXM [37], sparfloxacin onto SGO [55], and methylene blue dye onto reduced graphene oxide (rGO) [77] in aqueous media occurred through multiple stages with varying adsorption rates.

Table 2
Estimated values of the diffusion parameters of levofloxacin adsorption onto SGO in aqueous solution.

Parameters	$[Levofloxacin]_0$ (μmol/L)					Temperature (°C)			
	10	25	50	75	100	25	30	35	40
Film Diffusion Model									
$k_{fd} \times 10^{-3}$ (min^{-1})	23.50	27.50	37.40	37.10	30.40	37.40	38.60	37.60	37.50
R^2	0.9900	0.9233	0.9851	0.9851	0.9577	0.9851	0.9755	0.9753	0.9729
Intraparticle Diffusion Model									
k_{id1} (μmol/g $min^{0.5}$)	7.80	33.46	55.58	55.19	69.46	55.58	52.57	53.18	49.35
I_1 (μmol/g)	−3.34	−19.45	−32.72	2.28	33.36	−32.72	−9.77	4.11	28.07
R^2	0.9855	0.9908	0.9950	0.9990	0.9988	0.9950	0.9933	0.9990	0.9991
k_{id2} (μmol/g $min^{0.5}$)	2.44	3.71	11.85	21.32	22.00	11.85	11.28	9.93	8.69
I_2 (μmol/g)	14.45	80.34	125.85	137.22	208.46	125.85	137.33	151.82	167.91
R^2	0.9441	0.8460	0.9615	0.9330	0.9519	0.9615	0.9690	0.9750	0.9677
k_{id3} (μmol/g $min^{0.5}$)	0.5	0.49	0.47	1.05	1.19	0.74	0.42	0.52	0.34
I_3 (μmol/g)	32.06	105.17	219.10	297.39	370.54	219.10	226.25	229.01	238.13
R^2	0.9064	0.8158	0.8736	0.8421	0.8705	0.8736	0.6859	0.6485	0.7299

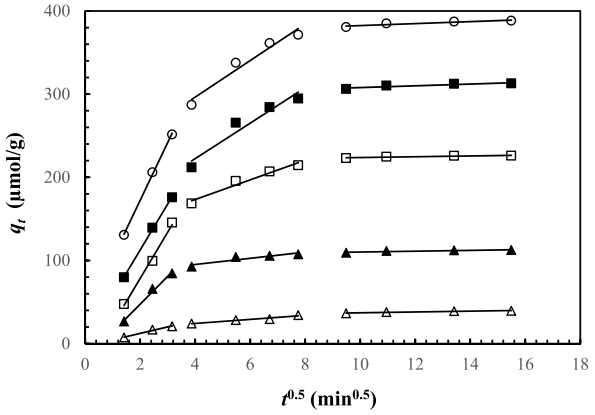

Fig. 8. Characteristic plots of q_t versus $t^{0.5}$ for the adsorption of levofloxacin onto SGO at different concentrations of levofloxacin (solution volume: 0.05 L; SGO: 0.010 g; temperature: 25 °C; pH: 4.0; ([Levofloxacin]$_0$: Δ: 10 µmol/L; ▲: 25 µmol/L; □: 50 µmol/L; ■: 75 µmol/L; ○: 100 µmol/L).

3.8. Activation parameters

Utilizing the k_2 values presented in Table 1, the activation energy for levofloxacin absorption onto SGO was computed. The activation energy (E_a) was estimated utilizing the formula given below [55]:

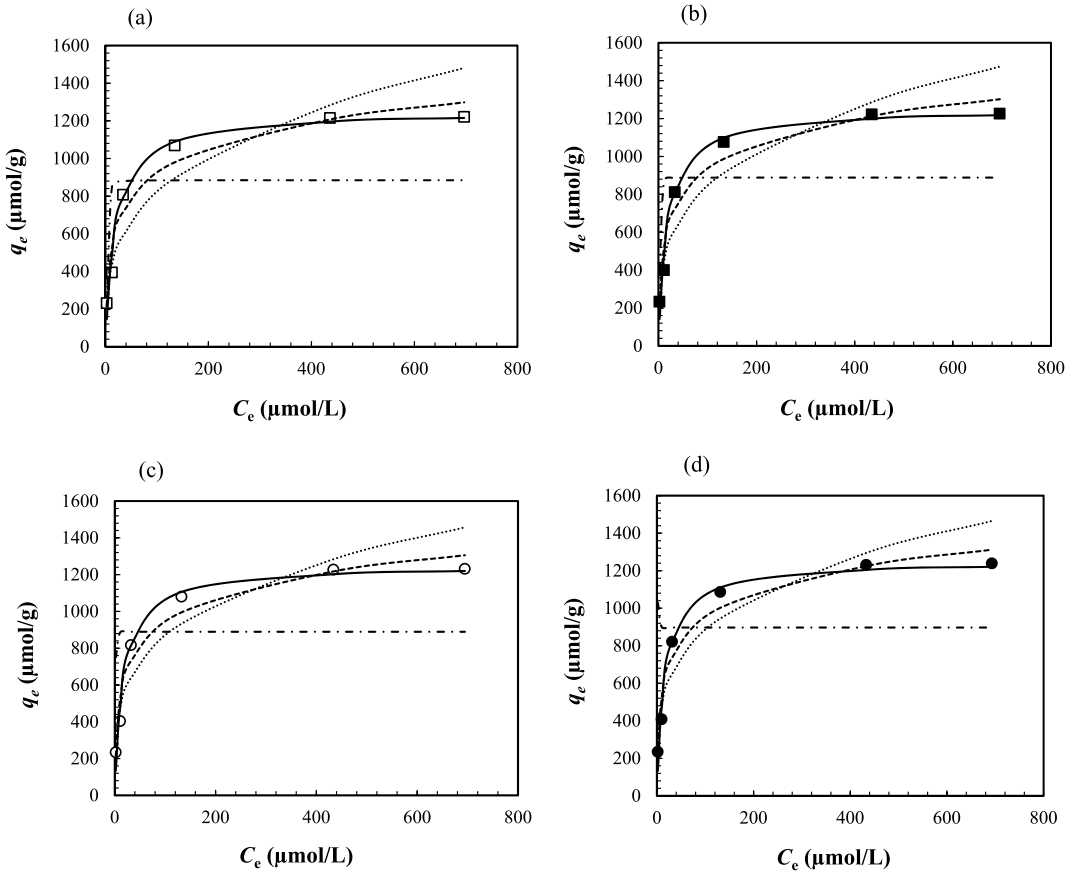

Fig. 9. Illustrates the equilibrium adsorption isotherm of levofloxacin onto SGO in aqueous solution (pH 4.0) at different temperatures (a) □: 25 °C; (b) ■: 30 °C; (c) ○: 35 °C; and (d) ●: 40 °C ([Levofloxacin]$_0$: 50–1000 µmol/L; solution volume: 0.05 L; SGO: 0.010 g). The Freundlich (…), Tempkin (—), Dubinin-Radushkevich (.-.-), and Langmuir isotherm (– –) equations and the values of isotherm constants (Table 3) were employed to simulate all lines.

$$\ln k_2 = -\frac{E_a}{RT} + constant \tag{13}$$

In this context, R signifies the universal gas constant with a value of 8.314 J/mol K. The activation energy (E_a) was determined to be 24.98 kJ/mol (Table 1) through calculation based on a plot of lnk_2 versus 1/T, yielding a coefficient of determination (R^2: 0.9988). The E_a value characterizes the relationship between the adsorbent and the adsorbate. The E_a values for physisorption and chemisorption are 5–40 kJ/mol and 40–800 kJ/mol, respectively. Therefore, the estimated E_a value (24.98 kJ/mol) suggests that the adsorption of levofloxacin onto SGO is predominantly a physisorption process, similar to the adsorption of sparfloxacin onto SGO in aqueous solution [55].

The changes in the enthalpy of activation ($\Delta H^{\ddagger}$), entropy of activation ($\Delta S^{\ddagger}$), and Gibbs free energy of activation ($\Delta G^{\ddagger}$) for levofloxacin absorption onto SGO were computed utilizing the following formulas [55]:

$$\ln\left(\frac{k_2}{T}\right) = -\frac{\Delta H^{\ddagger}}{RT} + \ln\frac{k_B}{h_P} + \frac{\Delta S^{\ddagger}}{R} \tag{14}$$

$$\Delta G^{\ddagger} = \Delta H^{\ddagger} - T\Delta S^{\ddagger} \tag{15}$$

In this context, k_2 (g/mol min) represents a rate constant of pseudo-second-order kinetic model, R stands for the universal gas constant (8.314 J/mol K), T denotes temperature in kelvins. h_P symbolizes the Planck constant (6.626×10^{-34} Js), and k_B represents the Boltzmann constant (1.381×10^{-23} J/K). The values of $\Delta H^{\ddagger}$ (22.45 kJ/mol; Table 1) and $\Delta S^{\ddagger}$ (−115.03 J/mol K; Table 1) were obtained by analyzing the slope and y-intercept of the graph plotting ln(k_2/T) versus 1/T (R^2 = 0.9985). The negative value of $\Delta S^{\ddagger}$ (−115.03 J/mol K) indicates that the levofloxacin molecules exhibited greater orderliness in the activated state and at the interface compared to the bulk solution phase [78]. Similar results were observed during the adsorptive removal of sparfloxacin by SGO and reactive red 239 dye by chitosan 8B in aqueous solutions [55,79]. The calculate $\Delta G^{\ddagger}$ values at 25, 30, 35, and 40 °C were computed to be 56.72, 57.30, 57.87 and 58.45 kJ/mol (Table 1), respectively. The positive values of ΔG indicate the presence of an energy barrier throughout the adsorption process. Comparable results were noted when sparfloxacin was adsorbed onto SGO and when reactive yellow 145 was adsorbed onto chitosan in aqueous environments [55,74].

3.9. Adsorption isotherm

Isotherm studies provide insights into the adsorption capacity and affinity between the adsorbent and adsorbate. In order to elucidate the adsorption mechanism, the experimental isotherm data were assessed utilizing common isotherm equations. Fig. 9 illustrates the relationship between q_e and C_e at various solution temperatures. The increase in the q_e value with increasing solution temperature (Fig. 9a–d) indicates that the adsorption of levofloxacin is an endothermic process, similar to the findings observed in the adsorption of sparfloxacin onto SGO [55].

The experimental isotherm data acquired at various temperatures were interpreted using Freundlich [80], Temkin [81], Dubinin–Radushkevich [82] and Langmuir [83] isotherm equations. The linear and non-linear versions of the isotherm equations are listed below.

Freundlich model:

$$\text{Nonlinear form } q_e = K_F C_e^{\frac{1}{n}} \tag{16}$$

$$\text{Linear form } ln\ q_e = \frac{1}{n} ln\ C_e + ln\ K_F \tag{17}$$

Temkin model:

$$\text{Nonlinear form} \quad q_e = \frac{RT}{b} ln(K_T C_e) \tag{18}$$

$$\text{Linear form } q_e = \frac{RT}{b} \ln K_T + \frac{RT}{b} ln\ C_e \tag{19}$$

Dubinin-Radushkevich model:

$$\text{Nonlinear form } q_e = q_{DR} \exp\left(-K_{DR}\varepsilon^2\right) \tag{20}$$

$$\text{Linear form } lnq_e = lnq_{DR} - K_{DR}\varepsilon^2 \tag{21}$$

$$\varepsilon = RT \ln\left(1 - \frac{1}{C_e}\right) \tag{22}$$

$$E = \frac{1}{(2K_{DR})^{0.5}} \tag{23}$$

Langmuir model:

$$\text{Nonlinear form } q_e = \frac{K_L C_e}{(1 + a_L C_e)} \tag{24}$$

$$\text{Linear form } \frac{C_e}{q_e} = \frac{1}{K_L} + \frac{a_L}{K_L} C_e \tag{25}$$

where C_e (μmol/L) represents the equilibrium concentration of levofloxacin in solution, q_e (μmol/g) represents the adsorbed quantity of levofloxacin per unit weight of SGO at equilibrium, K_F ((μmol/g) (μmol/L)$^{-1/n}$) and n are Freundlich constants associated with adsorption capacity and adsorption intensity, respectively [76]. K_T (μmol/L) denotes Temkin constant, b (J/mol) is a constant associated with heat of adsorption. ε denotes polanyi potential, E presents mean adsorption energy, K_{DR} denotes Dubinin-Radushkevich constant and q_{DR} is the maximum adsorption capacity. K_L (L/g) and a_L(L/μmol) are the Langmuir adsorption constants. The K_L/a_L ratio represents the capacity for maximal levofloxacin uptake, q_m (μmol/g). T and R carry the identical significance as stated previously. The isotherm constants were calculated using linear isotherm equations (figures not shown).

Table 3 presents the isotherm parameter values. The K_F values showed a positive correlation with increasing temperatures from 25 to 40 °C, indicating that levofloxacin uptake is an endothermic process. The n values were 3.27, 3.45, 3.72, and 3.80 at temperatures of 25, 30, 35, and 40 °C, respectively, suggesting a favorable adsorption process [55]. The K_T values (1.17 μmol/L, 1.33 μmol/L, 1.53 μmol/L, and 1.66 μmol/L) and b values (12.79 J/mol, 13.22 J/mol, 13.66 J/mol, and 13.98 J/mol) were determined at 25, 30, 35, and 40 °C, respectively, from the intercepts and slopes of the q_e vs. lnC_e plots (figure not provided). These b values confirmed that levofloxacin adsorption onto SGO was endothermic [55]. According to the Dubinin-Radushkevich model, the calculated E values were 0.71 kJ/mol, 1.12 kJ/mol, 2.89 kJ/mol, and 3.54 kJ/mol at 25, 30, 35, and 40 °C, respectively, indicating that levofloxacin adsorption onto SGO is primarily a physical adsorption process [55,62,65]. Comparing the RMSE and R^2 values (Table 3) from the Freundlich, Temkin, Dubinin-Radushkevich, and Langmuir models, it was concluded that the experimental isotherm data fit well with the Langmuir model. Furthermore, the experimental adsorption equilibrium data were compared to the isotherm data calculated using the Freundlich, Tempkin, Dubinin-Radushkevich, and Langmuir models (Fig. 9a–d). The characteristics of the observed adsorption isotherm data were accurately replicated by the simulated data from the Langmuir model, as illustrated in Fig. 9a–d. This supports the conclusion that the Langmuir equation effectively describes all the isotherm data. As shown in Table 3, the values of a_L and K_L increased as the solution temperature rose from 25 to 40 °C. These results suggest that the interaction between SGO and levofloxacin is likely an endothermic process [55]. The maximum uptake capacity (q_m) of levofloxacin on SGO was determined to be 1250 μmol/g at 25 °C using the Langmuir equation. Similar findings were observed in the adsorptive removal of sparfloxacin using SGO [55], as well as in the removal of Allura Red AC from aqueous solutions using sawdust treated with hexadecylpyridinium bromide [62].

Table 3
Isotherm and thermodynamic parameters for the adsorption of levofloxacin onto SGO at various temperatures.

Parameters	Temperatures (K)			
	298	303	308	313
Freundlich Isotherm Model				
K_F ((μmol/g) (μmol/L)$^{-1/n}$)	199.70	220.77	250.81	261.91
n	3.27	3.45	3.72	3.80
R^2	0.9144	0.9279	0.9441	0.9469
RMSE	175.07	166.01	153.38	152.23
Temkin Isotherm Model				
K_T (μmol/L)	1.17	1.33	1.53	1.66
b (J/mol)	12.79	13.22	13.66	13.98
R^2	0.9567	0.9598	0.9616	0.9643
RMSE	88.67	85.66	83.93	81.30
Dubinin-Radushkevich Isotherm Model				
q_{DR} (μmol/g)	884.30	888.38	889.63	896.95
$K \times 10^{-6}$ (J^2/mol^2)	1.00	0.40	0.06	0.04
E (kJ/mol)	0.71	1.12	2.89	3.54
R^2	0.6459	0.6457	0.6367	0.6456
RMSE	306.36	319.47	389.09	473.04
Langmuir Isotherm Model				
K_L (L/g)	62.89	68.03	72.46	75.76
$a_L \times 10^{-3}$ (L/μmol)	50.31	54.42	57.97	60.61
q_m (μmol/g)	1250.00	1250.00	1250.00	1250.00
R^2	0.9996	0.9996	0.9996	0.9997
RMSE	58.49	57.43	58.96	56.61
Thermodynamic Study				
ΔG (kJ/mol)	−26.82	−27.47	−28.09	−28.66
ΔH (kJ/mol)	9.66			
ΔS (J/mol K)	122.47			
R^2	0.9885			

Table 4 provides a comparative analysis of levofloxacin adsorption capacities between SGO and other adsorbents reported in the literature. SGO demonstrated a higher adsorption capacity than other adsorbents, including chitosan-walnut shells composite [24], magnetite (Fe_3O_4) nanoparticles [33], graphene oxide [36], FXM hydrogel [37], granular activated carbon [38], cellulose nanocrystals/graphene oxide [39], graphene nanoplatelets [40], rice husk biochar [41], and multi-walled carbon nanotubes [42]. Thus, it is recommended to use SGO for the economical and efficient removal of levofloxacin from aqueous environments.

3.10. Confirmation of levofloxacin adsorption onto SGO by FTIR, SEM and EDX

Fig. 10 shows the FTIR spectra of SGO before and after loading with levofloxacin. The broad peak at 3406 cm^{-1} for O–H stretching in SGO (Fig. 10a) shifted by 56 cm^{-1} to 3462 cm^{-1} after loading with levofloxacin (Fig. 10b), indicating an interaction between the O–H group of SGO and levofloxacin molecules. The peak at 1734 cm^{-1}, attributed to the carboxylic C=O group of SGO (Fig. 10a), shifted by 18 cm^{-1} to 1752 cm^{-1} in levofloxacin-loaded SGO (Fig. 10b). The sharp peak at 1624 cm^{-1} for C=C vibration in SGO (Fig. 10a) shifted to 1622 cm^{-1} in levofloxacin-loaded SGO (Fig. 10b). Additionally, two new bands appeared at 1446 and 1396 cm^{-1} in the spectrum of levofloxacin-loaded SGO (Fig. 10b). The peaks for C–O–C (1221 cm^{-1}), C–O (1053 cm^{-1}), and S–O (840 cm^{-1}) stretching vibrations in SGO (Fig. 10a) shifted to 1080, 975, and 827 cm^{-1}, respectively, after adsorption of levofloxacin onto SGO (Fig. 10b). The intensity of the characteristic SGO bands (O–H and C=O) decreased, while the C=C band intensity increased due to the interaction between SGO and levofloxacin (Fig. 10b). Similar observations were previously reported for norfloxacin adsorption onto GO [84]. These results confirm that levofloxacin effectively adsorbed onto SGO.

SEM was used to investigate the morphological features of SGO before and after adsorption of levofloxacin molecules. Fig. 11 illustrates the SEM images of untreated SGO and levofloxacin-loaded SGO. Before treatment with levofloxacin, the surface of SGO was irregular, rough, crumpled, and porous (Fig. 11a). In contrast, the relatively uniform and smooth surface of levofloxacin-loaded SGO (Fig. 11b) indicates effective adsorption of levofloxacin onto SGO.

Fig. 12 shows the EDX elemental compositions of SGO before and after adsorption of levofloxacin. Prior to the antibiotic adsorption, carbon, oxygen, and sulfur were present on the surface of SGO, while fluorine was not detected (Fig. 12a). After levofloxacin adsorption, the mass percentage of carbon on the surface of SGO increased, and fluorine was detected in the EDX spectrum of levofloxacin-loaded SGO (Fig. 12b). These results confirm that levofloxacin successfully adsorbed onto the surfaces of SGO.

3.11. Thermodynamics

Thermodynamic parameters, including changes in Gibb's free energy (ΔG, kJ/mol), enthalpy (ΔH, kJ/mol) and entropy (ΔS, J/mol K), were determined utilizing the subsequent equations [76]:

$$\Delta G = -RT \ln a_L \tag{26}$$

$$ln\, a_L = \frac{\Delta S}{R} - \frac{\Delta H}{RT} \tag{27}$$

The variables a_L, R, T, q_e, and C_e retain the same definitions as mentioned earlier in this paper. Enthalpy (ΔH) and entropy (ΔS) changes during the adsorption process were calculated from the slope and intercept of the $\ln a_L$ versus $1/T$ plot ($R^2 = 0.9885$). The results of the thermodynamic studies are presented in Table 3. The positive ΔH value (9.66 kJ/mol) indicates that the adsorption process is endothermic. Conversely, the negative ΔG values (−26.82 to −28.66 kJ/mol) suggest that the process is feasible and spontaneous. The positive ΔS value (122.47 J/mol K) signifies that levofloxacin molecules have a strong affinity for the SGO surface and experience increased randomness during the adsorption process. Similar observations were noted for the adsorption of sparfloxacin onto SGO in aqueous solution [55].

3.12. Desorption and reuse of SGO

Desorption and reusability of an adsorbent are indispensable for the development of a batch adsorption process that is both cost-

Table 4
Comparison of the adsorption capacities of different adsorbents for removing levofloxacin from an aqueous environment.

Adsorbents	pH	Temperature (°C)	$q_{m.}$ (μmol/g)	$q_{m.}$ (mg/g)	References
Chitosan-walnut shells composite	7	25	20.56	7.43	[24]
Magnetite (Fe_3O_4) nanoparticles	7	25	62.18	22.47	[33]
Graphene Oxide (GO)	5.6	25	710.08	256.6	[36]
FXM hydrogel	6.5	25	522.12	188.68	[37]
Granular activated carbon	9	30	277.78	100.38	[38]
Cellulose nanocrystals/graphene oxide	4	20	137.59	49.72	[39]
Graphene nanoplatelets	5	25	29.44	10.64	[40]
Rice husk biochar	8	30	13.81	4.99	[41]
Multi-walled carbon nanotubes	–	–	1.70	0.613	[42]
SGO	4	25	1250.00	451.71	Present Study

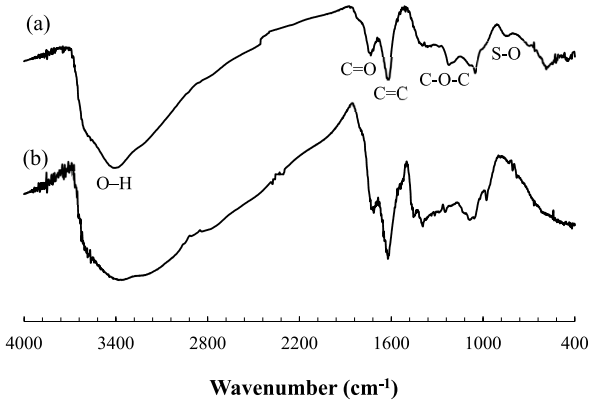

Fig. 10. FTIR spectra of SGO before (a) and after (b) adsorption of levofloxacin.

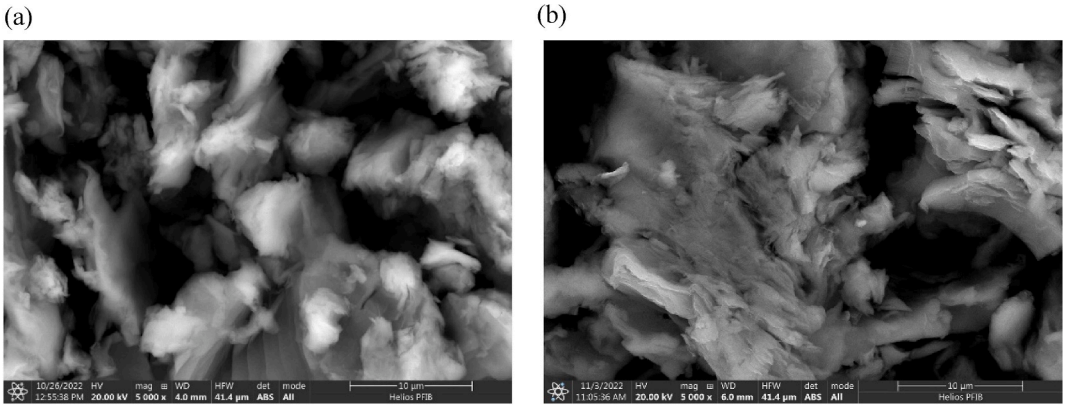

Fig. 11. SEM image of SGO before (a) and after (b) adsorption of levofloxacin.

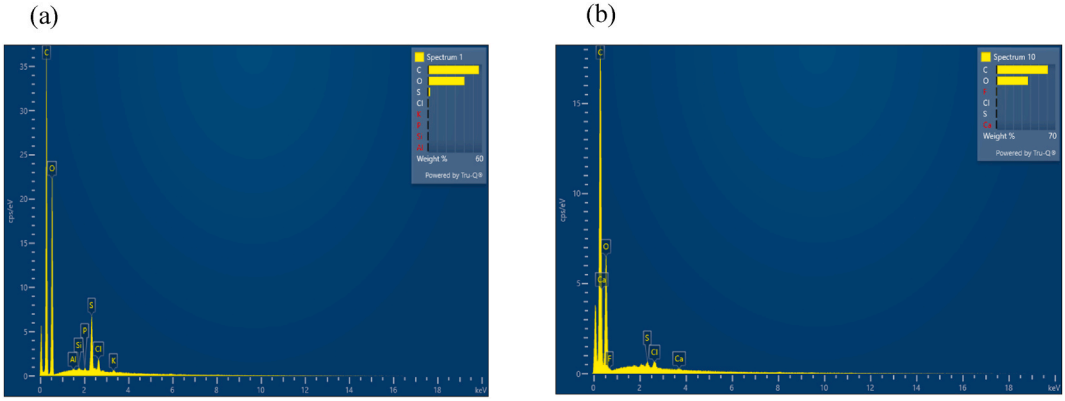

Fig. 12. EDX elemental spectra of SGO before (a) and after (b) adsorption of levofloxacin.

effective and efficient. To determine optimal conditions for desorbing levofloxacin from antibiotic-loaded SGO, several control desorption experiments were conducted:

(i) levofloxacin-loaded SGO in deionized water (H_2O);
(ii) levofloxacin-loaded SGO in methanol (MeOH);
(iii) levofloxacin-loaded SGO in ethanol (EtOH);

(iv) levofloxacin-loaded SGO in DMF;
(v) levofloxacin-loaded SGO in 1 mol/L HCl;
(vi) levofloxacin-loaded SGO in MeOH with 1 mol/L HCl;
(vii) levofloxacin-loaded SGO in EtOH with 1 mol/L HCl;
(viii) levofloxacin-loaded SGO in DMF with 1 mol/L HCl.

The progress of desorption was monitored using UV–vis spectroscopy by tracking the characteristic absorption peak of levofloxacin. The results, shown in Fig. 13, indicate the percentage of levofloxacin released from antibiotic-loaded SGO in various solvents over 240 min: H_2O (3.22 %), MeOH (2.38 %), EtOH (2.35 %), DMF (57.72 %), 1 mol/L HCl (39.32 %), 1 mol/L HCl in EtOH (36.63 %), 1 mol/L HCl in MeOH (58.55 %), and 1 mol/L HCl in DMF (99.82 %). These findings highlight that the most effective desorption occurred in 1 mol/L HCl in DMF. Preliminary screening confirmed that both 1 mol/L HCl and DMF are necessary for complete levofloxacin release from antibiotic-loaded SGO.

Fig. 14 shows the typical adsorption-desorption kinetics and changes in the adsorption capacity of regenerated SGO. The adsorption experiment was conducted using a 50 μmol/L solution of levofloxacin at 25 °C and pH 4.0. Levofloxacin desorption from the levofloxacin-loaded SGO was studied in a DMF solution with 1 mol/L HCl. During the initial adsorption phase (Fig. 14a), the equilibrium adsorption capacity of levofloxacin was found to be 227.12 μmol/g. A rapid desorption rate was observed (Fig. 14a), with 98.07 % of the loaded levofloxacin being released within 10 min. More than 99 % was released within 240 min. This could be due to the reduced electrostatic interaction between SGO and levofloxacin in the highly acidic DMF solution. Another reason might be the replacement of protonated levofloxacin molecules by hydronium ions (H_3O^+) in the acidic medium. Additionally, the methyl group ($-CH_3$) of DMF has a strong affinity for the hydrophobic segment of SGO, while the carbonyl group (C=O) of DMF interacts with the hydrophilic segment, aiding the release of levofloxacin molecules [85,86]. After the desorption stage, levofloxacin was readsorbed, showing similar adsorption behavior as during the initial phase (Fig. 14a). Similar levels of levofloxacin adsorption were observed during subsequent adsorption phases. This indicates that the SGO adsorbent can be reused effectively for removing levofloxacin from aqueous solutions. In the initial, first, second, third, fourth, and fifth regeneration cycles, the q_e values were 227.12, 226.26, 225.56, 225.04, 220.94, and 216.88 μmol/g, respectively (Fig. 14b). The gradual decrease in adsorption capacity could be due to pore blockage, reduced availability of active sites, and adsorbent depletion after each cycle [87]. Similar results were seen in the adsorption of sparfloxacin onto SGO in aqueous solutions [55]. These findings suggest that SGO could be used as an effective adsorbent for removing levofloxacin from aquatic environments.

4. Conclusions

The aim of this study was to investigate the efficiency of SGO in adsorbing and removing levofloxacin from aqueous environments. The results indicate that the adsorption process is significantly affected by the solution pH. The quantity of levofloxacin adsorbed onto SGO increased as the contact time, levofloxacin concentration, and solution temperature increased. Kinetic and isotherm analyses suggest that the adsorption mechanism follows the pseudo-second-order kinetic model and the Langmuir isotherm model. The maximum adsorption capacity of levofloxacin onto SGO was found to be 1250 μmol/g in aqueous solutions at pH 4 and 25 °C. Thermodynamic studies (ΔH: 9.66 kJ/mol; ΔS: 122.47 J/mol.K; and ΔG: −26.82 to −28.66 kJ/mol) indicate that the adsorption of levofloxacin onto SGO is spontaneous and endothermic. The E_a value of 24.98 kJ/mol indicates that the adsorption process is characteristic of physisorption. The initial desorption rate was rapid, with 99.62 % of the loaded levofloxacin released from the antibiotic-loaded SGO in DMF containing 1 mol/L HCl within 240 min. Five to six adsorption-desorption cycles were conducted to evaluate the reusability of SGO. Based on the experimental and calculated results, it can be concluded that SGO has a promising adsorption capacity for removing levofloxacin from aquatic environments.

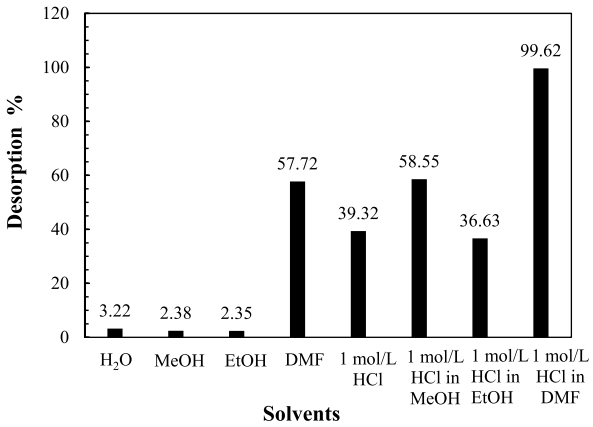

Fig. 13. Investigation of the desorption behavior of levofloxacin from levofloxacin-loaded SGO in different solvents.

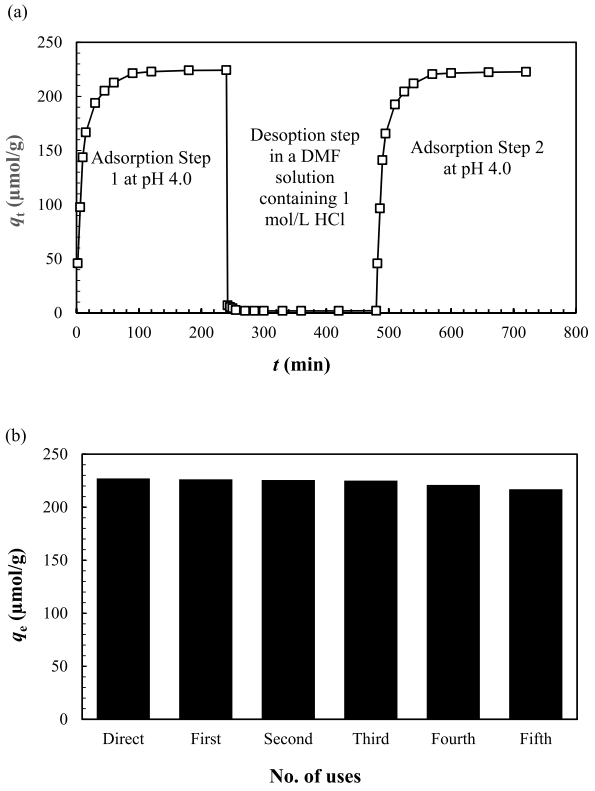

Fig. 14. (a) Kinetic graph of the cycle of levofloxacin adsorption and desorption at 25 °C and 50 µmol/L levofloxacin with three steps: adsorption step 1 at initial pH 4.0, desorption step in a DMF solution containing 1 mol/L HCl, and adsorption step 2 at initial pH 4.0. (b) The impact of regeneration cycles on the adsorption capacity of levofloxacin at standard conditions (50 µmol/L levofloxacin, 0.05 L solution volume, 0.01 g SGO, 25 °C temperature, pH 4.0).

CRediT authorship contribution statement

Chironjit Kumar Shaha: Writing – original draft, Methodology, Investigation, Formal analysis, Data curation,. **Subarna Karmaker:** Writing – review & editing, Supervision, Project administration, Funding acquisition, Conceptualization. **Tapan Kumar Saha:** Writing – review & editing, Supervision, Project administration, Funding acquisition, Conceptualization.

Declaration of competing interest

The authors declare the following financial interests/personal relationships which may be considered as potential competing interests:Tapan Kumar Saha reports financial support was provided by Alexander von Humboldt Foundation. Not Applicable If there are other authors, they declare that they have no known competing financial interests or personal relationships that could have appeared to influence the work reported in this paper.

Acknowledgments

We sincerely appreciate the assistance provided by the Alexander von Humboldt Foundation (ref.34-8151/T.K.S. (GA-Nr. 20 007)) in Germany and the Ministry of Science and Technology, Government of the People's Republic of Bangladesh (T.K.S. and S.K.). We also thank the Wazed Miah Science Research Center, Jahangirnagar University, for allowing us to analyze the samples using FTIR, and Md Abdullah Al Mahmud, a PhD student in the Department of Chemistry at Louisiana State University, Baton Rouge, LA 70803, USA, for analyzing the samples using SEM and EDX analyzer systems.

References

[1] Z. Maghsodian, A.M. Sanati, T. Mashifana, M. Sillanpää, S. Feng, T. Nhat, B. Ramavandi, Occurrence and distribution of antibiotics in the water, sediment, and biota of freshwater and marine environments: a review, Antibiotics 11 (2022) 1461.

[2] J. Wang, L. Chu, L. Wojnárovits, E. Takács, Occurrence and fate of antibiotics, antibiotic resistant genes (ARGs) and antibiotic resistant bacteria (ARB) in municipal wastewater treatment plant: an overview, Sci. Total Environ. 744 (2020) 140997.

[3] N.H. Tran, M. Reinhard, K.Y.H. Gin, Occurrence and fate of emerging contaminants in municipal wastewater treatment plants from different geographical regions-a review, Water Res. 133 (2018) 182–207.
[4] U. Szymańska, M. Wiergowski, I. Sołtyszewski, J. Kuzemko, G. Wiergowska, M.K. Woźniak, Presence of antibiotics in the aquatic environment in Europe and their analytical monitoring: recent trends and perspectives, Microchem. J. 147 (2019) 729–740.
[5] M. Anwar, Q. Iqbal, F. Saleem, Improper disposal of unused antibiotics: an often overlooked driver of antimicrobial resistance, Expert Rev. Anti Infect. Ther. 18 (2020) 697–699.
[6] M.T. Khan, I.A. Shah, I. Ihsanullah, M. Naushad, S. Ali, S.H.A. Shah, A.W. Mohammad, Hospital wastewater as a source of environmental contamination: an overview of management practices, environmental risks, and treatment processes, J. Water Process Eng. 41 (2021) 101990.
[7] C. Manyi-Loh, S. Mamphweli, E. Meyer, A. Okoh, Antibiotic use in agriculture and its consequential resistance in environmental sources: potential public health implications, Molecules 23 (2018) 795.
[8] V. Economou, P. Gousia, Agriculture and food animals as a source of antimicrobial-resistant bacteria, Infect. Drug Resist. 8 (2015) 49–61.
[9] P. Taylor, R. Reeder, Antibiotic use on crops in low and middle-income countries based on recommendations made by agricultural advisors, CABI Agric. Biosci. 1 (2020) 1.
[10] F.C. Cabello, H.P. Godfrey, A.H. Buschmann, H.J. Dölz, Aquaculture as yet another environmental gateway to the development and globalisation of antimicrobial resistance, Lancet Infect. Dis. 16 (2016) e127–e133.
[11] D.J. Larsson, C. de Pedro, N. Paxeus, Effluent from drug manufactures contains extremely high levels of pharmaceuticals, J. Hazard Mater. 148 (2007) 751–755.
[12] J. Fick, H. Söderström, R.H. Lindberg, C. Phan, M. Tysklind, D.J. Larsson, Contamination of surface, ground, and drinking water from pharmaceutical production, Environ. Toxicol. Chem. 28 (2009) 2522–2527.
[13] D.G. Joakim Larsson, Pollution from drug manufacturing: review and perspectives, Philos. Trans. R. Soc. Lond. B Biol. Sci. 369 (2014) 20130571.
[14] A.I. Samreen, H. Malak, H.H. Abulreesh, Environmental antimicrobial resistance and its drivers: a potential threat to public health, J. Glob. Antimicrob. Resist. 27 (2021) 101–111.
[15] J.W.F. Wu-Wu, C. Guadamuz-Mayorga, D. Oviedo-Cerdas, W.J. Zamora, Antibiotic resistance and food safety: perspectives on new technologies and molecules for microbial control in the food industry, Antibiotics 12 (2023) 550.
[16] G.J. Noel, A review of levofloxacin for the treatment of bacterial infections, Clin. Med. Therapeut. 1 (2009). CMT. S28.
[17] A. Sitovs, I. Sartini, M. Giorgi, Levofloxacin in veterinary medicine: a literature review, Res. Vet. Sci. 137 (2021) 111–126.
[18] D.N. Fish, A.T. Chow, The clinical pharmacokinetics of levofloxacin, Clin. Pharmacokinet. 32 (1997) 101–119.
[19] A.R. Mahmood, H.H. Al-Haideri, F.M. Hassan, Detection of antibiotics in drinking water treatment plants in Baghdad City, Iraq, Adv. Public Health 2019 (2019) 7851354.
[20] G. Ghosh, S. Hanamoto, N. Yamashita, X. Huang, H. Tanaka, Antibiotics removal in biological sewage treatment plants, Pollution 2 (2016) 131–139.
[21] M.B. Cristóvão, S. Tela, A.F. Silva, M. Oliveira, A. Bento-Silva, M.R. Bronze, M.T.B. Crespo, J.G. Crespo, M. Nunes, V.J. Pereira, Occurrence of antibiotics, antibiotic resistance genes and viral genomes in wastewater effluents and their treatment by a pilot scale nanofiltration unit, Membranes 11 (2020) 9.
[22] Z. Zhou, Z. Zhang, L. Feng, J. Zhang, Y. Li, T. Lu, H. Qian, Adverse effects of levofloxacin and oxytetracycline on aquatic microbial communities, Sci. Total Environ. 734 (2020) 139499.
[23] G. Zhu, W. Li, P. Wang, G. Cheng, L. Chen, K. Zhang, X. Li, One-step polymerization of hydrophilic ionic liquid imprinted polymer in water for selective separation and detection of levofloxacin from environmental matrices, J. Separ. Sci. 43 (2020) 639–647.
[24] A.E.D. Mahmoud, M. Fawzy, Decontamination of levofloxacin from water using a novel chitosan–walnut shells composite: linear, nonlinear, and optimization modeling, Appl. Water Sci. 13 (2023) 244.
[25] A. Orzoł, A.I. Piotrowicz-Cieślak, Levofloxacin is phytotoxic and modifies the protein profile of lupin seedlings, Environ. Sci. Pollut. Res. 24 (2017) 22226–22240.
[26] A. Kaur, D.B. Salunke, A. Umar, S.K. Mehta, A. Sinha, S.K. Kansal, Visible light driven photocatalytic degradation of fluoroquinolone levofloxacin drug using Ag_2O/TiO_2 quantum dots: a mechanistic study and degradation pathway, New J. Chem. 41 (2017) 12079–12090.
[27] G. Lu, Z. Lun, H. Liang, H. Wang, Z. Li, W. Ma, In situ fabrication of $BiVO_4$-$CeVO_4$ heterojunction for excellent visible light photocatalytic degradation of levofloxacin, J. Alloys Compd. 772 (2019) 122–131.
[28] H. Wei, D. Hu, J. Su, K. Li, Intensification of levofloxacin sono-degradation in a US/H_2O_2 system with Fe_3O_4 magnetic nanoparticles, Chin. J. Chem. Eng. 23 (2015) 296–302.
[29] S. Adhikari, S. Mandal, D.H. Kim, Z-scheme 2D/1D MoS_2 nanosheet-decorated $Ag_2Mo_2O_7$ microrods for efficient catalytic oxidation of levofloxacin, Chem. Eng. J. 373 (2019) 31–43.
[30] J. Lyu, M. Ge, Z. Hu, C. Guo, One-pot synthesis of magnetic $CuO/Fe_2O_3/CuFe_2O_4$ nanocomposite to activate persulfate for levofloxacin removal: investigation of efficiency, mechanism and degradation route, Chem. Eng. J. 389 (2020) 124456.
[31] C. Guo, H. Liu, C. Wang, J. Zhao, W. Zhao, N. Lu, J. Qu, X. Yuan, Y.N. Zhang, Electrochemical removal of levofloxacin using conductive graphene/polyurethane particle electrodes in a three-dimensional reactor, Environ. Pollut. 260 (2020) 114101.
[32] K.O. Iwuozor, Prospects and challenges of using coagulation-flocculation method in the treatment of effluents, Adv. J. Chem. A 2 (2019) 105–127.
[33] S. Altaf, R. Zafar, W.Q. Zaman, S. Ahmad, K. Yaqoob, A. Syed, A.J. Khan, M. Bilal, M. Arshad, Removal of levofloxacin from aqueous solution by green synthesized magnetite (Fe_3O_4) nanoparticles using Moringa olifera: kinetics and reaction mechanism analysis, Ecotoxicol. Environ. Saf. 226 (2021) 112826.
[34] P. Ghosh, S. Saha, R.K. Bishwas, S. Karmaker, T.K. Saha, Adsorption of amaranth onto natural peanut husk and cationic surfactant-modified peanut husk in aqueous solution: kinetic, isotherm, and thermodynamic analysis, Cellul. Chem. Technol. 56 (2022) 443–460.
[35] S. Chowdhury, P. Ghosh, MdT.R. Joy, S. Karmaker, T.K. Saha, Adsorption characteristics of amaranth onto cetyltrimethylammonium bromide (CTAB)-modified rice husk in aqueous solution, Colloid J. 84 (2022) 196–207.
[36] S. Dong, Y. Sun, J. Wu, B. Wu, A.E. Creamer, B. Gao, Graphene oxide as filter media to remove levofloxacin and lead from aqueous solution, Chemosphere 150 (2016) 759–764.
[37] N. Rahman, A. Raheem, Mechanistic investigation of levofloxacin adsorption on Fe(III)-tartaric acid/xanthan gum/graphene oxide/polyacrylamide hydrogel: Box-Behnken design and Taguchi method for optimization, J. Ind. Eng. Chem. 127 (2023) 110–124.
[38] T.M. Darweesh, M.J. Ahmed, Batch and fixed bed adsorption of levofloxacin on granular activated carbon from date (Phoenix dactylifera L.) stones by KOH chemical activation, Environ. Toxicol. Pharmacol. 50 (2017) 159–166.
[39] J. Tao, J. Yang, C. Ma, J. Li, K. Du, Z. Wei, C. Chen, Z. Wang, C. Zhao, X. Deng, Cellulose nanocrystals/graphene oxide composite for the adsorption and removal of levofloxacin hydrochloride antibiotic from aqueous solution, R. Soc. Open Sci. 7 (2020) 200857.
[40] A. Zakaa, T.H. Ibrahima, M.I. Khamisb, N.A. Jabbara, Experimental design modelling and optimization of levofloxacin removal with graphene nanoplatelets using response surface method, Desalination Water Treat. 169 (2019) 38–48.
[41] S. Yi, B. Gao, Y. Sun, J. Wu, X. Shi, B. Wu, X. Hu, Removal of levofloxacin from aqueous solution using rice-husk and wood-chip biochars, Chemosphere 150 (2016) 694–701.
[42] I. Kariim, A. Abdulkareem, O. Abubakre, Development and characterization of MWCNTs from activated carbon as adsorbent for metronidazole and levofloxacin sorption from pharmaceutical wastewater: kinetics, isotherms and thermodynamic studies, Sci. Afr. 7 (2020) e00242.
[43] R. Rostamian, H. Behnejad, A comparative adsorption study of sulfamethoxazole onto graphene and graphene oxide nanosheets through equilibrium, kinetic and thermodynamic modeling, Process Saf. Environ. Protect. 102 (2016) 20–29.
[44] H. Chen, B. Gao, H. Li, Removal of sulfamethoxazole and ciprofloxacin from aqueous solutions by graphene oxide, J. Hazard Mater. 282 (2015) 201–207.
[45] K. Sun, S. Dong, Y. Sun, B. Gao, W. Du, H. Xu, J. Wu, Graphene oxide-facilitated transport of levofloxacin and ciprofloxacin in saturated and unsaturated porous media, J. Hazard Mater. 348 (2018) 92–99.
[46] D. Huang, X. Wang, C. Zhang, G. Zeng, Z. Peng, J. Zhou, M. Cheng, R. Wang, Z. Hu, X. Qin, Sorptive removal of ionizable antibiotic sulfamethazine from aqueous solution by graphene oxide-coated biochar nanocomposites: influencing factors and mechanism, Chemosphere 186 (2017) 414–421.

[47] N. Ninwiwek, P. Hongsawat, P. Punyapalakul, P. Prarat, Removal of the antibiotic sulfamethoxazole from environmental water by mesoporous silica-magnetic graphene oxide nanocomposite technology: adsorption characteristics, coadsorption and uptake mechanism, Colloids Surf. A Physicochem. Eng. Asp. 580 (2019) 123716.
[48] T. Van Tran, D.T.C. Nguyen, H.T. Le, D.-V.N. Vo, S. Nanda, T.D. Nguyen, Optimization, equilibrium, adsorption behavior and role of surface functional groups on graphene oxide-based nanocomposite towards diclofenac drug, J. Environ. Sci. 93 (2020) 137–150.
[49] M.F. Li, Y.G. Liu, G.M. Zeng, S.B. Liu, X.J. Hu, D. Shu, L.H. Jiang, X.F. Tan, X.X. Cai, Z.I. Yan, Tetracycline absorbed onto nitrilotriacetic acid-functionalized magnetic graphene oxide: influencing factors and uptake mechanism, J. Colloid Interface Sci. 485 (2017) 269–279.
[50] A. Ashiq, M. Vithanage, B. Sarkar, M. Kumar, A. Bhatnagar, E. Khan, Y. Xi, Y.S. Ok, Carbon-based adsorbents for fluoroquinolone removal from water and wastewater: a critical review, Environ. Res. 197 (2021) 111091.
[51] S. Thangavel, G. Venugopal, Understanding the adsorption property of graphene-oxide with different degrees of oxidation levels, Powder Technol. 257 (2014) 141–148.
[52] M.P. Wei, H. Chai, Y.I. Cao, D.Z. Jia, Sulfonated graphene oxide as an adsorbent for removal of Pb^{2+} and methylene blue, J. Colloid Interface Sci. 524 (2018) 297–305.
[53] A. Tawfik, M. Eraky, M.N. Khalil, A.I. Osman, D.W. Rooney, Sulfonated graphene nanomaterials for membrane antifouling, pollutant removal, and production of chemicals from biomass: a review, Environ. Chem. Lett. 21 (2023) 1093–1116.
[54] F. Shoushtarian, M.R.A. Moghaddam, E. Kowsari, Efficient regeneration/reuse of graphene oxide as a nanoadsorbent for removing basic Red 46 from aqueous solutions, J. Mol. Liq. 312 (2020) 113386.
[55] C.K. Shaha, M.A.A. Mahmud, S. Saha, S. Karmaker, T.K. Saha, Efficient removal of sparfloxacin antibiotic from water using sulfonated graphene oxide: kinetics, thermodynamics, and environmental implications, Heliyon 10 (2024) e33644.
[56] D.C. Marcano, D.V. Kosynkin, J.M. Berlin, A. Sinitskii, Z. Sun, A. Slesarev, L.B. Alemany, W. Lu, J.M. Tour, Improved synthesis of graphene oxide, ACS Nano 4 (2010) 4806–4814.
[57] G.M.S. Uddin, S. Saha, S. Karmaker, T.K. Saha, Adsorption of cefixime trihydrate onto chitosan 10b from aqueous solution: kinetic, equilibrium and thermodynamic studies, Cellul. Chem. Technol. 55 (2021) 771–784.
[58] H. Zhang, H. Selim, Kinetics of arsenate adsorption−desorption in soils, Environ. Sci. Tech. 39 (2005) 6101–6108.
[59] X. Zhang, J. Shen, N. Zhuo, Z. Tian, P. Xu, Z. Yang, W. Yang, Interactions between antibiotics and graphene-based materials in water: a comparative experimental and theoretical investigation, ACS Appl. Mater. Interfaces 8 (2016) 24273–24280.
[60] I. Ahmad, R. Bano, M.A. Sheraz, S. Ahmed, T. Mirza, S.A. Ansari, Photodegradation of levofloxacin in aqueous and organic solvents: a kinetic study, Acta Pharm. 63 (2013) 223–229.
[61] Y. Zhou, S. Cao, C. Xi, X. Li, L. Zhang, G. Wang, Z. Chen, A novel Fe_3O_4/graphene oxide/citrus peel-derived bio-char based nanocomposite with enhanced adsorption affinity and sensitivity of ciprofloxacin and sparfloxacin, Bioresour. Technol. 292 (2019) 121951.
[62] T.K. Saha, R.K. Bishwas, S. Karmaker, Z. Islam, Adsorption characteristics of Allura red AC onto sawdust and hexadecylpyridinium bromide-treated sawdust in aqueous solution, ACS Omega 5 (2020) 13358–13374.
[63] X.S. Wang, J.P. Chen, Removal of the azo dye Congo red from aqueous solutions by the marine alga *Porphyra yezoensis* Ueda, Clean–Soil, Air, Water 37 (2009) 793–798.
[64] H. Shi, W. Li, L. Zhong, C. Xu, Methylene blue adsorption from aqueous solution by magnetic cellulose/graphene oxide composite: equilibrium, kinetics, and thermodynamics, Ind. Eng. Chem. Res. 53 (2014) 1108–1118.
[65] S. Karmaker, A.J. Nag, T.K. Saha, Adsorption of remazol brilliant violet onto chitosan 10B in aqueous solution: kinetics, equilibrium and thermodynamics studies, Cellul. Chem. Technol. 53 (2019) 373–386.
[66] T.K. Saha, N.C. Bhoumik, S. Karmaker, M.G. Ahmed, H. Ichikawa, Y. Fukumori, Adsorption characteristics of reactive black 5 from aqueous solution onto chitosan, Clean–Soil, Air, Water 39 (2011) 984–993.
[67] V. Sabna, S.G. Thampi, S. Chandrakaran, Adsorptive removal of cationic and anionic dyes using graphene oxide, Water Sci. Technol. 78 (2018) 732–742.
[68] K. Yang, B. Chen, X. Zhu, B. Xing, Aggregation, adsorption, and morphological transformation of graphene oxide in aqueous solutions containing different metal cations, Environ. Sci. Technol. 50 (2016) 11066–11075.
[69] C.K. Shaha, B. Sarker, S.K. Mahalanobish, M.S. Hossain, S. Karmaker, T.K. Saha, Kinetics, equilibrium, and thermodynamics for conjugation of chitosan with insulin-mimetic [meso-Tetrakis (4-sulfonatophenyl) porphyrinato] oxovanadate (IV)(4−) in an aqueous solution, ACS Omega 8 (2023) 41612–41623.
[70] S. Pervin, C.K. Shaha, S. Karmaker, T.K. Saha, Conjugation of insulin-mimetic [meso-tetrakis (4-sulfonatophenyl) porphyrinato] zinc (II) with chitosan in aqueous solution: kinetics, equilibrium and thermodynamics, Polym. Bull. 78 (2021) 4527–4550.
[71] S. Lagergren, Zur theorie der sogenannten adsorption geloster stoffe, Kungliga svenska vetenskapsakademiens, Handlingar 24 (1898) 1–39.
[72] Y.S. Ho, G. McKay, Pseudo-second order model for sorption processes, Process Biochem 34 (1999) 451–465.
[73] S.Y. Elovich, O. Larionov, Theory of adsorption from nonelectrolyte solutions on solid adsorbents: 2. Experimental verification of the equation for the adsorption isotherm from solutions, Bull. Acad. Sci. USSR, Div. Chem. Sci. 11 (1962) 198–203.
[74] S. Karmaker, T. Sen, T.K. Saha, Adsorption of reactive yellow 145 onto chitosan in aqueous solution: kinetic modeling and thermodynamic analysis, Polym. Bull. 72 (2015) 1879–1897.
[75] W.J. Weber Jr., J.C. Morris, Kinetics of adsorption on carbon from solution, J. Sanit. Eng. Div. 89 (1963) 31–59.
[76] C. Duran, D. Ozdes, A. Gundogdu, H.B. Senturk, Kinetics and isotherm analysis of basic dyes adsorption onto almond shell (Prunus dulcis) as a low cost adsorbent, J. Chem. Eng. Data 56 (2011) 2136–2147.
[77] F.A. Arias, M. Guevara, T. Tene, P. Angamarca, R. Molina, A. Valarezo, O. Salguero, C. Vacacela Gomez, M. Arias, L.S. Caputi, The adsorption of methylene blue on eco-friendly reduced graphene oxide, Nanomaterials 10 (2020) 681.
[78] E. Eren, Adsorption performance and mechanism in binding of azo dye by raw bentonite, Clean–Soil, Air, Water 38 (2010) 758–763.
[79] S. Karmaker, F. Sintaha, T.K. Saha, Kinetics, isotherm and thermodynamic studies of the adsorption of reactive red 239 dye from aqueous solution by chitosan 8B, Adv. Biol. Chem. 9 (2019) 1–22.
[80] H. Freundlich, Adsorption solution, J. Phys. Chem 57 (1906) 384–470.
[81] M. Temkin, Kinetics of ammonia synthesis on promoted iron catalysts, Acta physiochim. URSS 12 (1940) 327–356.
[82] Q. Hu, Z. Zhang, Application of Dubinin–Radushkevich isotherm model at the solid/solution interface: a theoretical analysis, J. Mol. Liq. 277 (2019) 646–648.
[83] I. Langmuir, The adsorption of gases on plane surfaces of glass, mica and platinum, J. Am. Chem. Soc. 40 (1918) 1361–1403.
[84] V.R. Moreira, Y.A.R. Lebron, M.M. da Silva, L.V. de Souza Santos, R.S. Jacob, C.K.B. de Vasconcelos, M.M. Viana, Graphene oxide in the remediation of norfloxacin from aqueous matrix: simultaneous adsorption and degradation process, Environ. Sci. Pollut. Res. 27 (2020) 34513–34528.
[85] X. Xing, H. Qu, R. Shao, Q. Wang, H. Xie, Mechanism and kinetics of dye desorption from dye-loaded carbon (XC-72) with alcohol-water system as desorbent, Water Sci. Technol. 76 (2017) 1243–1250.
[86] X. Xing, H. Qu, P. Chen, B. Chi, H. Xie, Studies on competitive adsorption of dyes onto carbon (XC-72) and regeneration of adsorbent, Water Sci. Technol. 74 (2016) 2505–2514.
[87] J. Yang, S. Shojaei, S. Shojaei, Removal of drug and dye from aqueous solutions by graphene oxide: adsorption studies and chemometrics methods, NPJ Clean Water 5 (2022) 5.